

# ROADM System for Space Division Multiplexing with Spatial Superchannels

M. D. Feuer<sup>1</sup>, L. E. Nelson<sup>1</sup>, K. Abedin<sup>2</sup>, X. Zhou<sup>1</sup>, T.F. Taunay<sup>2</sup>, J. F. Fini<sup>2</sup>, B. Zhu<sup>2</sup>, R. Isaac<sup>1</sup>, R. Harel<sup>3</sup>, G. Cohen<sup>3</sup>, and D. M. Marom<sup>4</sup>

<sup>1</sup>AT&T Labs - Research, Middletown, NJ, USA ([mdfeuer@att.com](mailto:mdfeuer@att.com))

<sup>2</sup>OFS Labs, Somerset, NJ, USA; <sup>3</sup>Oclaro, Inc, Denville, NJ, USA; <sup>4</sup>Hebrew University of Jerusalem, Jerusalem, Israel.

**Abstract:** A two-span SDM system includes the first ROADM supporting spatial superchannels and the first cladding-pumped multicore-EDFA directly spliced to multicore transmission fiber. For  $6 \times 40 \times 128$ -Gb/s SDM-WDM-PDM-QPSK transmission, BER penalties are  $\leq 1.6$  dB in Add, Drop, and Express paths.

**OCIS codes:** (060.2330) Fiber optics communications; (060.2360) Fiber optics links and subsystems

## 1. Introduction

Research in space-division multiplexing (SDM) has yielded dramatic increases in transmission capacity per fiber, using multiple modes in multimode fiber [1-2], multiple cores in multicore fiber (MCF) [3-5], or multiple modes in multiple cores [6]. However, capacity is only part of the picture; to achieve commercial success, SDM must offer lower cost-per-bit and must support photonic routing at reconfigurable optical add/drop (ROADM) nodes as well. Only when these requirements have been met can a transitional strategy be initiated.

Spatial superchannels, in which high-rate (e.g., 1Tb/s) data streams are transported as groups of subchannels occupying the same wavelength in separate modes/cores, can help lower the cost of transceivers through component sharing and simplified DSP [7]. Since all of the subchannels are routed together through the network, the approach also enables cost-effective ROADMs, in which a single switching element is used to route all of the subchannels belonging to a single superchannel.

Optical amplifiers for multi-span SDM systems must achieve the same beneficial cost scaling as transceivers and ROADMs, prompting research into multicore erbium-doped fiber amplifiers (MC-EDFAs) [8,9]. To take best advantage of MC-EDFA technology, such amplifiers should be connected directly to MCF transmission spans, without breakout devices to single-mode fiber at the amplifier inputs and outputs.

In this paper, we present the first demonstration of a two-span ROADM transmission system adapted for spatial superchannel routing. The ROADM subsystem comprises two 23-port wavelength-selective switches (WSSs), with 18 fiber ports configured to support full Add/Drop/Express routing of 6 cores simultaneously, using only one steering mirror per wavelength in each WSS. At the ROADM input, a cladding-pumped MC-EDFA [8] is directly spliced to the MCF of the first transmission span. This direct splice eliminates the cost and complexity of the breakout device used in prior MC-EDFA experiments [9], a major step towards useful SDM technology. The two-span system was used to transport 40 C-band wavelengths of  $6 \times 128$  Gb/s each, and bit-error ratio (BER) was measured for Add, Drop and Express paths.

## 2. Experiment

Fig. 1 illustrates the operating principle of a  $7 \times (1 \times 2)$  WSS. Input signals from ports 1 through 7 reach the steering mirror at varying angles. Depending on the mirror tilt, the beams are jointly steered to either ports 7a through 7b or to ports 1b through 7b. (Within a WSS, wavelengths are separated by a dispersive element (e.g., a diffraction grating) and sent to separate steering mirrors, effectively replicating the pattern of Fig. 1 for each wavelength.) For this work, we adjusted the port assignments and the

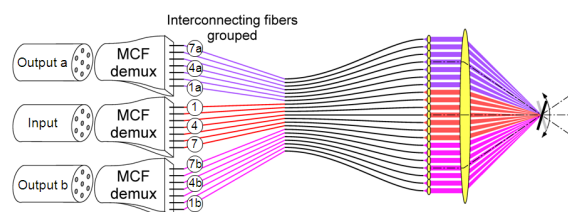


Fig. 1. Operating principle of  $7 \times (1 \times 2)$  WSS.

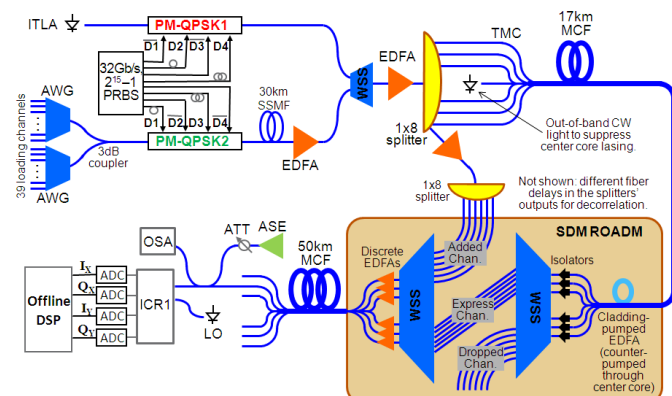


Fig. 2. Experimental setup.

mirror tilt angles of a commercial  $1 \times 23$  WSS with MEMS mirrors for steering and a layer of liquid-crystal (LC) cells for controlled attenuation. The WSS channel spacing of 50GHz matched that of our WDM signals.

Our experimental diagram is shown in Fig. 2. The channel-under-test originates from an integrated tunable laser assembly (ITLA), whose output is sent to an integrated, polarization-multiplexed, quadrature modulator, driven with XI, XQ, YI, YQ tributaries at 32Gb/s to create a polarization-multiplexed quadrature phase-shift-keyed (PM-QPSK) data stream at 128 Gb/s. Delays and inversions of the 32Gb/s electrical data signals are used to assure decorrelation of the I and Q data sequences in both polarizations. A WSS combines this channel with a 50-GHz spaced comb of 39 loading channels, also modulated with 128Gb/s PM-QPSK data and then transmitted through 30km of fiber for WDM channel decorrelation. An erbium-doped fiber amplifier (EDFA) and a  $1 \times 8$  power splitter prepare the combined signals for launch into the first MCF span. A tapered multicore coupler (TMC) guides the single-mode signals into the six outer cores of a 17-km, 7-core MCF span, similar to that used in [10], which is directly spliced to a cladding-pumped MC-EDFA similar to the one described in [8]. A tapered region at the splice location improves the matching of the transmission span core pitch to that of the MC-EDFA. A 30m length of seven-core EDF with a core diameter of 3.2  $\mu\text{m}$  and a core pitch of 40  $\mu\text{m}$  comprises the MC-EDFA, which was cladding-pumped with light from a multi-mode 980nm laser via the center core of a special TMC. This precluded use of the center core of the MC-EDF to carry data. A CW-laser at 1562.5nm was input to the center core of the 17-km transmission span to suppress spontaneous lasing in the center core of the MC-EDFA.

At the MC-EDF output, the second TMC splits out the cores to single-mode fibers to connect to the first of the two WSSs making up the ROADM subsystem. The WSS ports are connected as shown in Fig. 1 to accomplish the simultaneous Add, Drop or Express path for all cores. Signals for the Add path are provided by amplifying and splitting the output from one remaining port of the first  $1 \times 8$  splitter. After the MCF ROADM, discrete EDFAs boost the signal power before a third TMC at the input of the second MCF span. After the 50 km MCF span, a final TMC restores the signals to single-mode fibers for ASE addition and detection by an integrated coherent receiver (ICR) (21 GHz bandwidth) with a second ITLA as local oscillator. The ICR includes polarization diverse optical hybrids and four sets of high sensitivity balanced photodiodes with four differential linear amplifiers. The receivers' outputs are digitized by a four-channel real-time oscilloscope with 80GSa/s sampling rate and 33GHz analog bandwidth and processed offline to compute BER over  $\sim 1.6 \times 10^6$  bits of information for each spatial subchannel.

Frequencies of the 40 channels ranged from 191.95 to 193.90 THz, and the launch powers into the TMCs for the first span and for the second span were set at -11 dBm/ch and +5dBm/ch, respectively. The estimated loss of the module comprising the first MCF transmission span, the MC-EDFA background loss, and associated TMC's, tapers and splices was  $\sim 11$ -21 dB, suggesting that considerable improvement is possible. The loss of the second span, including its TMCs, ranged from 18.8 dB to 23.3 dB for the various cores. The loss of each WSS was  $\leq 5$ dB, and an additional attenuation of 7 dB was used in the second WSS to avoid overdriving the booster EDFAs.

The digital signal processing for the receiver is described in [7, 11].

### 3. Results and Discussion

Fig. 3 shows the net gain of the assembly made up of the 17-km MCF span, the MC-EDFA, and associated tapered splices, as a function of optical frequency. As noted in [8], pumping efficiency of the cladding-pumped MC-EDFA was relatively low, limiting output power per core and requiring operation under conditions of strong gain compression. Therefore, the gain and noise figure of the MC-EDFA were better at lower frequencies. Gain tilt is as high as 7 dB in the core with the lowest-loss input splice (and thus the highest input power and strongest gain compression). OSNR is more constant over frequency, but is generally lower for cores with high values of input loss. Power equalization among frequencies was implemented by adjusting the attenuation of the 'Drop' WSS, while equalization among subchannels (cores) was achieved by adjusting the gain of the ROADM post-amplifiers.

Fig. 4 compares the insertion losses and passband widths of the SDM ROADM for all 6 subchannels, when the ROADM is set for Express (i.e., two WSS in tandem) with minimum attenuation. For both parameters, the

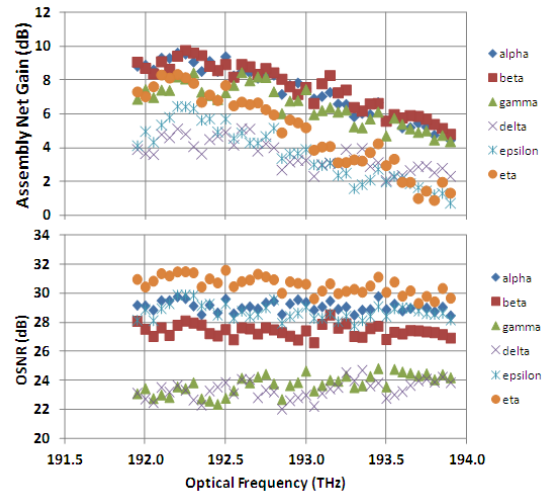


Fig. 3. Gain & OSNR for each core of the assembly comprising the 17-km MCF span, the MC-EDFA and all associated tapers, splices, and TMCs.

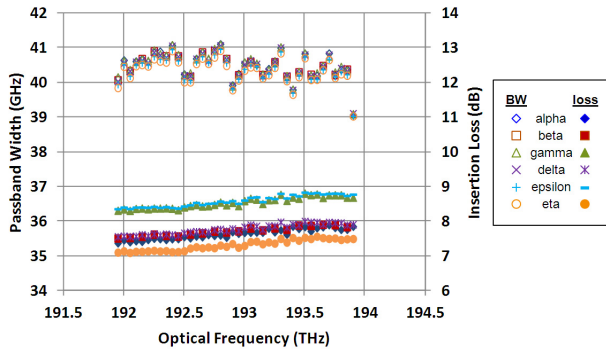


Fig. 4. ROADM passband width and insertion loss for the Express path for all six subchannels. The ‘gamma’ and ‘epsilon’ connections follow the nominal paths of the input WSS and the output WSS, respectively.

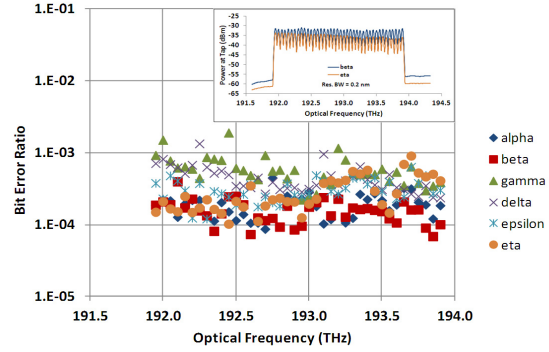


Fig. 5. For the Express path without added ASE, BER  $< 2 \times 10^{-3}$  is observed for all wavelengths in all cores. The inset shows the received power spectra for the highest-power and the lowest power cores.

subchannels are well-matched, showing no significant penalty in the ancillary connections directed by each mirror that are used to support spatial subchannels.

We have also measured BER for all 40 channels and all cores for the express path at maximum OSNR condition, yielding the results shown in Fig. 5. As expected, the cores with the best OSNR after the MC-EDFA (i.e., cores alpha and beta) show the lowest BER, but BER for all cores and all wavelengths remains well below the threshold of  $2 \times 10^{-2}$  expected for strong FEC with 24% coding overhead. The inset of Fig. 5 shows received power spectra for cores beta and eta, which are the highest-power and lowest-power cores, respectively.

Fig. 6 shows BER measurements for the lowest frequency channel ( $f=191.95$  THz) as a function of received OSNR for Drop, Add, and Express paths. For all cores, the OSNR penalties at  $1 \times 10^{-2}$  BER (compared to a back-to-back measurement with the same transmitter and receiver) were  $< 0.5$  dB,  $< 0.9$  dB, and  $< 0.9$  dB, respectively, for the Drop, Add and Express paths. BER vs. OSNR measurements were also made for all cores at the maximum frequency ( $f=193.90$  THz) and the center frequency ( $f=192.95$  THz), and OSNR penalties  $< 1.6$  dB were observed.

#### 4. Conclusion

We have demonstrated transmission and routing of 6core $\times$ 40 $\lambda$  $\times$ 128-Gb/s SDM-WDM-PDM-QPSK signals in a two-span, 67-km, MCF system including a ROADM adapted for spatial superchannels, and measured its BER performance. A cladding-pumped multicore-EDFA was directly spliced to the first MCF transmission span, obviating the need for a pair of MCF-to-SMF breakout devices. The WSS-based ROADM successfully steered six spatial subchannels with each of its mirror elements, enabling full Add/Drop/Express capability for all wavelengths.

We gratefully acknowledge Sheryl Woodward and Peter Magill of AT&T Labs and D. J. DiGiovanni of OFS Labs for their advice and support.

#### 5. References

- [1] Ip, E. et al., ECOC 2011, paper Th.13.C.2 (2011).
- [2] Sleiffer, V. A. J. M. et al., ECOC 2012, postdeadline paper Th.3.C.4 (2012).
- [3] Sakaguchi, J. et al., OFC-NFOEC 2012, paper PDP5C (2012).
- [4] Gnauck, A.H. et al., ECOC 2012, paper Th.2.C.2 (2012).
- [5] Takara, H. et al., ECOC 2012, postdeadline paper Th3.C.1 (2012).
- [6] Qian, D. et al., Frontiers in Optics 2012, postdeadline paper FW6C.3 (2012).
- [7] Feuer, M. et al., Phot. Technol. Lett. 24,1957-1960 (2012).
- [8] Abedin, K. et al., Opt. Express 20(18), 20191- 20200 (2012).
- [9] Takahashi, H. et al., ECOC 2012, postdeadline paper Th.3.C.3 (2012).
- [10] Zhu, B. et al., OFC-NFOEC 2011, paper PDPB7 (2011).
- [11] Zhou, X. et al, J. Lightwave Technol. 29, 571-577 (2011).

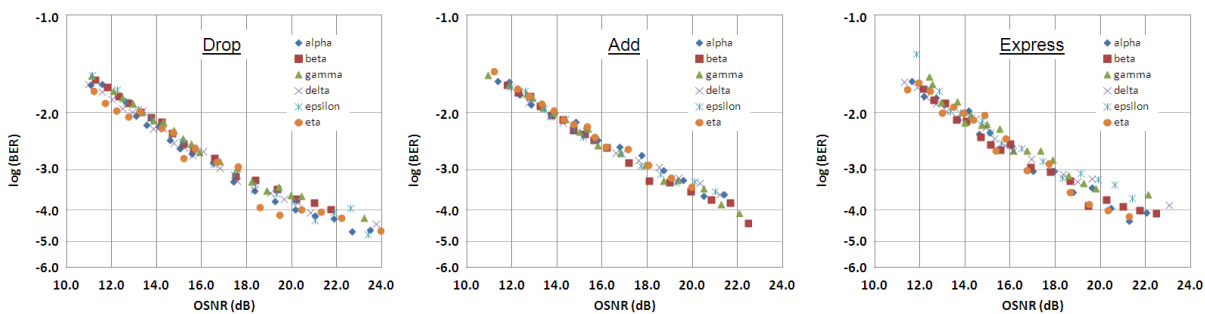


Fig. 6. BER as a function of OSNR for Drop (17km), Add (50km), and Express (67km) paths, all six cores,  $f=191.95$  THz.